Ceramics International 42 (2016) 16084–16089

Contents lists available at ScienceDirect

Ceramics International

journal homepage: www.elsevier.com/locate/ceramint

Nickel-based catalyst derived from NiO–$Ce_{0.75}Zr_{0.25}O_2$ nanocrystalline composite: Effect of the synthetic route on the partial oxidation of methane

V.R. da Silveira [a], D.M.A. Melo [a], B.S. Barros [b,*], J.A.C. Ruiz [c], Leopoldo O. Alcazar Rojas [c]

[a] Federal University of Rio Grande do Norte, Institute of Chemistry, PO BOX 1662, Natal, RN, 59078-970 Brazil
[b] Federal University of Pernambuco, Department of Mechanical Engineering, Recife, PE, 50070-901 Brazil
[c] Center for Gas Technology and Renewable Energy – CTGAS-ER, Av. Capitão-Mor Gouveia, 1480, Lagoa Nova, Natal, RN, 59063-40 Brazil

ARTICLE INFO

Article history:
Received 12 June 2016
Accepted 18 July 2016
Available online 19 July 2016

Keywords:
Syngas
Partial oxidation of methane
Pechini
Self-combustion
Microwave

ABSTRACT

In this work, we investigated the effects of two different synthetic routes, Pechini and microwave-induced combustion method, on the properties of nickel-based catalysts derived from NiO-$Ce_{0.75}Zr_{0.25}O_2$ nanocomposite. Powder samples were characterized by specific surface area (SSA) via BET method, X-ray diffraction (XRD), scanning electron microscopy (SEM) and temperature-programmed reduction (TPR). It was found that the synthesis method has a significant influence on the powder morphology, which may affect the catalytic activity. The nickel-based catalysts were tested for the partial oxidation of methane showing high CH_4 conversion, 80% and 81% after the first hour on stream, for the samples prepared by Pechini and combustion method, respectively. These samples also exhibited catalytic stability, keeping CH_4 conversion levels about 77% and 80% after ten hours on stream, respectively. We suggest that such good performance is related to the good dispersion and particle size of the metallic nickel over Zr-CeO2 support.

1. Introduction

Partial oxidation of methane (POM) is an attractive route to involve methane into the synthesis of liquid fuel and valuable chemicals [1,2]. The primary product of POM is a mixture of H_2 and CO, known as synthesis gas (syngas), with H_2/CO molar ratio of 2 suitable for the production of methanol and Fisher-Tropsch synthesis [3]. Noble metals are extensively reported as highly active and stable catalysts for partial oxidation of methane, particularly Ru [4–8]. However, the high cost limits their application at industrial scale.

Nickel catalysts supported on alumina are traditionally used for syngas production from methane via dry reforming [9], steam reforming [10] and partial oxidation [11]. Despite their high activity and low cost, these catalysts show a major drawback due to fast deactivation caused by coke deposition, sintering of the nickel particles or both. Therefore, development of more active and stable catalysts has become an important task over the last decades. The selection and modification of the catalytic support have been proposed as a practical approach to developing nickel-based catalysts with high activity and good stability. It is known that a healthy interaction between the active phase and the support with high oxygen mobility can reduce the coke deposition, as well as sintering effects [12]. Mixed oxides with fluorite-type structure Zr-CeO_2 appears like a good alternative. In fact, the addition of Zr to CeO_2 improves the oxygen storage capacity, the redox property, the thermal resistance of CeO_2 and it allows a better metal dispersion [13–15]. These properties may be influenced by the preparation method. Song et al. [16] reported the enhancement of the coke resistance in Ni/Al_2O_3 catalyst when prepared by a modified sol-gel method using glycerol. Chen et al. [17] studied the effect of preparation methods on structure and performance of Ni/$Ce_{0.75}Zr_{0.25}O_2$ catalyst for dry methane reforming. In general, many methods have been applied in the synthesis of oxides, as well as of heterogeneous catalysts, including the microwave-assisted combustion and the Pechini method. Probably, these two approaches are the most used routes to synthesize oxide materials with different types of properties [18–21].

The Pechini method is a low-temperature synthesis technique based on a solution polymerization route. This synthetic route has been widely used to synthesize mixed oxides due to its low cost and versatility. Compared to conventional solid-state reaction methods, the Pechini method provides the obtaining of powders

* Corresponding author.
E-mail address: braulio.barros@ufpe.br (B.S. Barros).

http://dx.doi.org/10.1016/j.ceramint.2016.07.119
0272-8842/

with high level of chemical homogeneity and more uniform particle size distribution [20,22].

Microwave-assisted combustion synthesis is presented here as an alternative to the conventional self-combustion method. In this synthetic approach, the interaction between the microwaves and the molecules in the precursor solution provides the heat necessary to launch the self-combustion reaction. Therefore, the heating is uniform, and high temperatures are reached faster, which can lead to different microstructures. Also, since the heating is instantaneous, microwave power provides a way to control the time and intensity of the reaction [9].

The effect of the synthetic route over structural and morphological properties of $Ce_{0.75}Zr_{0.25}O_2$ and NiO-$Ce_{0.75}Zr_{0.25}O_2$ compounds was studied. Furthermore, the catalytic performance of the nickel-based compounds was evaluated in the partial oxidation of methane.

2. Experimental details

2.1. Synthesis of $Ce_{0.75}Zr_{0.25}O_2$ solid solution

Cerium nitrate [$Ce(NO_3)_3 \cdot 6H_2O$, ALDRICH], zirconium oxynitrate [$ZrO(NO_3)_2 \cdot xH_2O$, NEON], nickel nitrate [$Ni(NO_3)_2 \cdot 6H_2O$, ALDRICH], urea [CH_4N_2O, VETEC], anhydrous citric acid [$C_6H_8O_7$, VETEC] and ethylene glycol [$C_2H_6O_2$, VETEC] were used as purchased without further purification.

In a typical synthesis via Pechini method, metallic nitrates, and citric acid were mixed in distilled water in a molar ratio of 1:3 (metallic ions: citric acid). This solution was stirred vigorously for 30 min at 70 °C. Then, ethylene glycol was added in a ratio of 40:60 in relation to the citric acid and the solution was kept under stirring for 120 min at 90 °C. At this temperature, polyesterification reactions, and water evaporation take place leading to the formation of a polymeric resin. This resin was heat-treated at 150 °C for 1 h (5 °C/min) and after at 300 °C for 4 h (5 °C/min) resulting in a fluffy black mass, which was subsequently ground to produce the polymeric precursor. Finally, the polymeric precursor was calcined at 800 °C for 4 h (5 °C/min) producing crystalline powders.

The same compound was prepared by microwave-induced combustion method using urea as fuel. The method introduced by Jain et al. [7] was used to calculate the amounts of each reagent, metallic nitrates, and urea. The values in moles for urea was calculated for a stoichiometric condition "$\phi = 1$". All reactants were dissolved in a minimum amount of water kept under stirring on a heating plate for 30 min at 70 °C. After that, the Beaker with the aqueous solution was transferred to a microwave oven with an output power of 700 W and frequency of 2.45 GHz. The precursor solution was exposed to microwaves until the spontaneous ignition takes place. The resulting powder was calcined under air atmosphere at 800 °C for 4 h.

2.2. Preparation of the nickel-based catalyst precursor

NiO-$Ce_{0.75}Zr_{0.25}O_2$ nanocrystalline composite was prepared by a wet impregnation method. The samples prepared previously by both mentioned synthetic routes were used as raw materials in this step. In each case, a known amount of powder was added to an aqueous nickel nitrate solution to form an aqueous suspension. This suspension was kept under stirring until the complete evaporation of water. The resulting product was dried at 150 °C for 2 h in a muffle furnace. Then, the samples were calcined in air flux (50 mL/min) at 900 °C for 4 h. It was used 15 wt% of Ni in relation to the amount of $Ce_{0.75}Zr_{0.25}O_2$.

The $Ce_{0.75}Zr_{0.25}O_2$ samples received the following nomenclature: CP for the sample prepared by the Pechini method and CC for the sample obtained by the self-combustion approach. The NiO-$Ce_{0.75}Zr_{0.25}O_2$ nanocrystalline composites received similar nomenclature: NCP, when derived from the powder prepared by Pechini method and NCC when derived from the powder obtained by self-combustion.

2.3. Characterization techniques

The structural characterization of the prepared powders was performed via X-ray diffraction (XRD) analysis using a diffractometer Shimadzu XRD-7000, operating with Cu-Kα radiation ($\lambda_{Cu} = 1.542$ Å). Patterns were collected in the 2θ range from 20° to 80° at a scan rate of 1.20°/min. The crystallite size was estimated by using the Scherrer equation and leading account the full width at half maximum of the diffraction peaks. Also, the Rietveld method was used for microstructural and quantitative analysis by using MAUD (Material Analysis Using Diffraction) program package version 2.55 [23]. The specific surface area was determined by the BET method using Micromeritics apparatus, model ASAP 2020 equipped with a thermal conductivity detector. The morphology of the powder samples was analyzed by scanning electron microscopy (SEM) on a Shimadzu SSX 550 microscope. Temperature-programmed reduction (TPR) measurements were carried out in the Autochem II Micromeritics apparatus. In a typical procedure, the samples (25 mg) were previously dehydrated at 150 °C (10 °C/min) for 30 min in an N_2 flow (50 mL/min). After cooling to 50 °C, the gas flow was changed to a mixture of 10% of H_2 in N_2 (50 mL/min) and the temperature increased up to 1000 °C (10 °C/min). The hydrogen consumption was monitored by a quadrupole mass spectrometer. Nickel-based catalysts were tested in the Partial oxidation of methane (POM). Experiments were carried out in the same apparatus previously described for the TPR analysis. To avoid hot spot formation or temperature gradients, 20 mg of each sample was diluted in 100 mg of quartz. Before the reaction, the catalyst was reduced in 10% H_2/N_2 (10 °C/min) at 900 °C for 10 min. Next, the temperature was decreased to 800 °C under N_2 atmosphere. A reactant mixture with CH_4: O_2 ratio of 2:1 (total flow of 100 mL/min) was used. The exit gasses were analyzed along time using a gas chromatograph (TRACE CG-Ultra). The catalytic performances were evaluated by CH_4 conversion, H_2/CO molar ratio, and selectivities towards CO and CO_2 calculated as follows:

$$Conversion\ (CH_4)(\%) = \frac{(CH_4)_{in} - (CH_4)_{out}}{(CH_4)_{in}} \times 100 \quad (1)$$

$$H_2/CO\ molar\ ratio = \frac{(H_2)_{out}}{(CO)_{out}} \quad (2)$$

$$Selectivity\ (CO)(\%) = \frac{(CO)_{out}}{(CH_4)_{in} - (CH_4)_{out}} \times 100 \quad (3)$$

$$Selectivity\ (CO_2)(\%) = \frac{(CO_2)_{out}}{(CH_4)_{in} - (CH_4)_{out}} \times 100 \quad (4)$$

3. Results and discussion

3.1. Structural and textural characterization

XRD analyses were performed for the samples prepared by

Table 1
Lattice parameters, atomic coordinates and site occupancy.

Lattice Parameters[a]	Coordinates[a]				
Zr-CeO_2	Atom	X	Y	Z	Occupancy
$a=b=c=5.3848$ Å	Ce	0.000	0.000	0.000	0.75
$\alpha=\beta=\gamma=90°$	Zr	0.000	0.000	0.000	0.25
	O	0.250	0.250	0.250	1.00
NiO	Atom	X	Y	Z	Occupancy
$a=b=c=4.1826$ Å	Ni	0.000	0.000	0.000	1.00
$\alpha=\beta=\gamma=90°$	O	0.500	0.500	0.500	1.00

[a] Adapted from COD files.

both microwave-assisted combustion and Pechini method, as well as to the samples with and without nickel. In all cases, Zr-CeO_2 solid solution crystallizes in a cubic fluorite-type structure with space group Fm-3m, according to Crystallography Open Database (COD) file number 210-2846. The diffraction peaks observed at 28.9°, 33.2°, 47.6°, 56.7°, 59.4°, 69.8°, 77.2° and 79.4° (2θ) are indexed to the crystallographic planes (111), (200), (202), (311), (222), (400), (313) and (402), respectively. Furthermore, nickel-containing compounds show four additional diffraction peaks due to the presence of the NiO cubic crystalline phase. The peaks observed at 37.3°, 43.3°, 62.9° and 75.4° (2θ) are indexed to the crystallographic planes (111), (200), (202) and (311), respectively, according to COD file number 432-0488.

XRD data were used for microstructural and quantitative analysis via Rietveld method. The instrumental contribution to the asymmetry and broadening of the diffraction peaks was calculated from a CeO_2 sample with high crystallinity. The crystallographic data available in the COD files were used as initial input parameters for the refinement performed in MAUD program package (Table 1). The background of each pattern was fitted by a sixth order polynomial function while the peak profile analysis was carried out considering isotropic behavior by using the Delft model [24]. The Rietveld refinement plots are shown in Fig. 1. Good agreement is observed between experimental profiles and the calculated structural model.

In Table 2 are presented the specific surface area data obtained by BET method and the numerical results from Rietveld refinement. For all samples were reached Rwp smaller that 18% and Sig between 1.09 and 1.27, confirming the quality of the refinement. By inspecting the results, it can be seen that samples prepared by the Pechini method show higher surface area and smaller average crystallite size than samples synthesized by self-combustion. This behavior is associated with the maximum temperature reached during the synthesis process, and it can be observed for both crystalline phases. It is well known that a higher temperature of processing can lead to the increasing the crystallite size and decrease the specific surface area. Furthermore, the microcrystalline strain is stronger for the samples prepared by Pechini method.

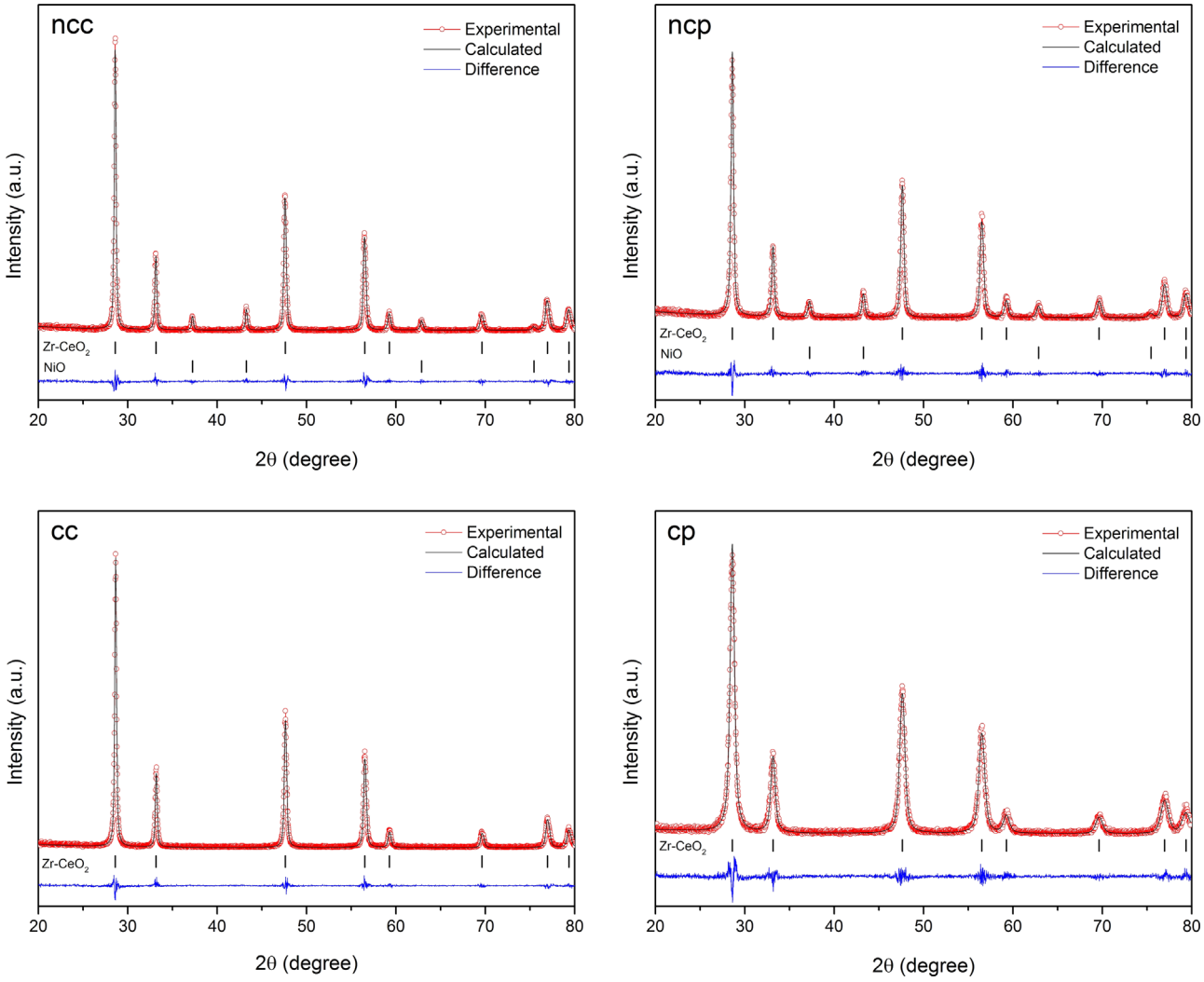

Fig. 1. Rietveld refinement plots of the prepared samples.

Table 2
Specific surface area (SSA) obtained by BET method and Rietveld refinement results: phase content (Wt), average crystallite size (D_{XRD}), microstrain ($\langle\epsilon^2\rangle^{1/2}$) and quality refinement indices, Sig and Rw_p.

Sample	SSA (m^2/g)	Wt (%)		D_{XRD} (nm)		$\langle\epsilon^2\rangle^{1/2}$ (10^{-4})		Sig	R_{wp} (%)
		$ZrCeO_2$	NiO	$ZrCeO_2$	NiO	$ZrCeO_2$	NiO		
CP	42	100	–	23	–	26.2489	–	1.20	16.2
CC	6	100	–	68	–	9.89969	–	1.18	16.0
NCP	18	78.2	21.8	49	43	15.2141	12.4333	1.27	17.4
NCC	6	82.7	17.3	83	79	11.2391	1.6707	1.09	14.0

Especially for NiO, the microcrystalline strain is about seven times larger for NCP when compared to NCC. Finally, the quantitative phase analysis reveals a composition close to the expected value, calculated with bases on the nominal composition (about 19 wt% of NiO).

3.2. Scanning electron microscopy analysis

The morphological characteristics of the produced powders were inspected by SEM analysis (Fig. 2). It is evident the effect of the synthesis method on the morphology. In Fig. 2a, it can be seen the typical morphology of the sample prepared by the Pechini method, which is characterized by hard agglomerates with sizes of up to 100 μm. It is worth to note the superficial rugosity of the agglomerate, which could indicate the presence of small crystallites, pores or both.

Sample CC presented the typical morphology of powders prepared by self-combustion method (Fig. 2b). It is possible to see sponge-like agglomerates with pores in micrometric scale. The windows on top-right of the respective figures show the area delimited by the white squares and these images had their contrast enhanced to make clear the morphological aspects. The same procedure was performed for the other figures. As can be seen, pores in sample CC are larger than those observed in the sample CP. It is known that larger pores contribute little to the specific surface area (SSA), what is in agreement with the results of SSA obtained by BET method presented in Table 2.

The impregnation of these samples with nickel nitrate followed by calcination at 900 °C did not change the morphological characteristics of the Zr-CeO_2 phase. However, a new crystalline phase (NiO) was formed, as previously confirmed by XRD data. SEM micrographs of NCP and NCC are depicted in Fig. 2c and d, respectively. In the NCP sample, NiO is formed on the surface of the Zr-CeO_2 agglomerates or as a free phase. On the other hand, in the NCC sample, NiO is formed mainly into the pores.

3.3. Temperature-programmed reduction

H_2-TPR profiles of the prepared samples are displayed in Fig. 3. As can be seen, reduction of Ce^{4+} to Ce^{3+} in CC and CP samples is a process carried out in three steps. The window on top-right shows the CC and CP profiles in a maximized scale. It is noticed that sample CC does not show the first reduction event at 433 °C and the second event is slightly shifted to 495 °C, compared to sample CP. On the other hand, the third reduction event occurs at a

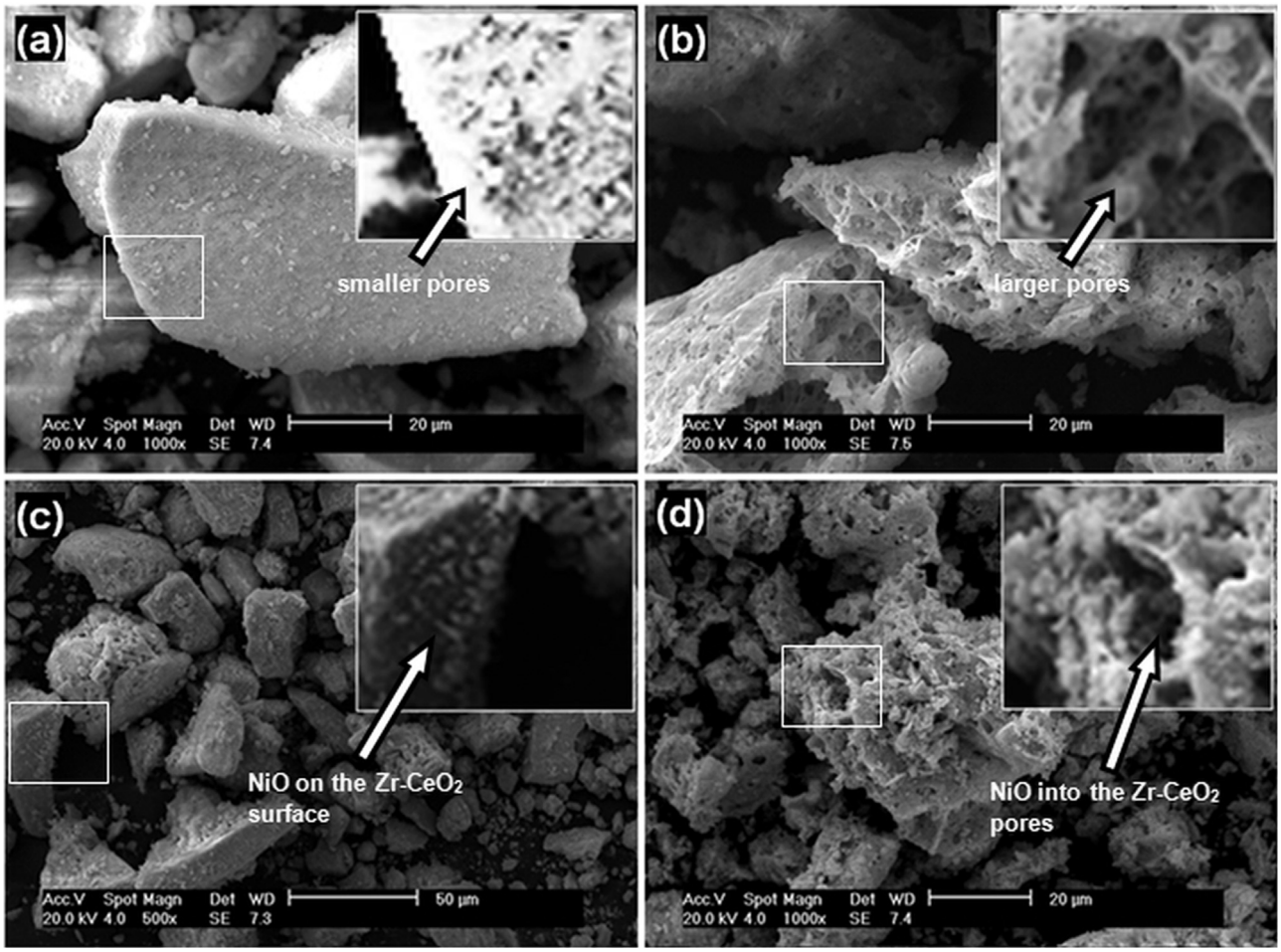

Fig. 2. SEM micrographs of the samples (a) CP, (b) CC, (c) NCP and (d) NCC.

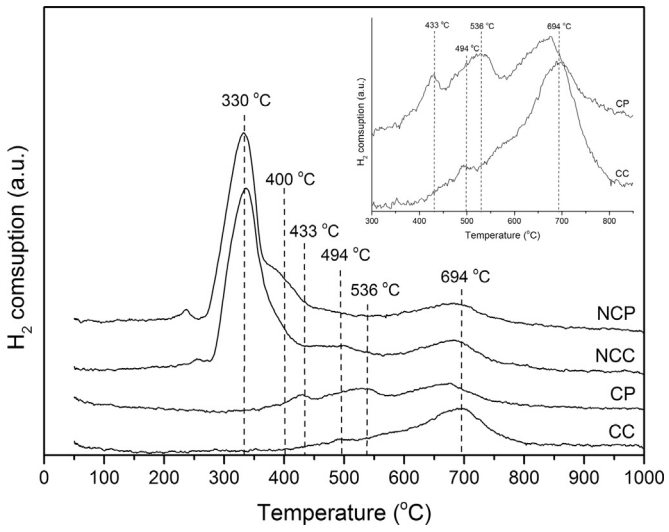

Fig. 3. H_2-TPR profiles of the prepared samples.

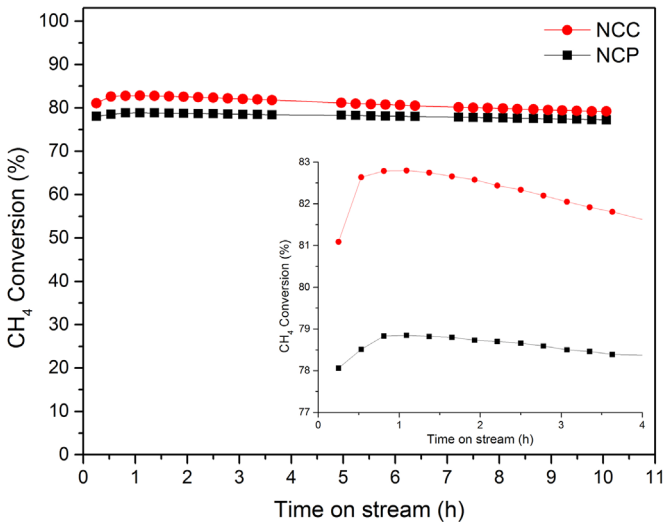

Fig. 4. CH_4 conversion profiles obtained as a function of the time on stream at 800 °C.

higher temperature (694 °C) in sample CC compared to CP. It is assumed that the reduction of Ce^{4+} to Ce^{3+} in fluorite-type compounds occurs via reduction of cerium on the surface (low-temperature peaks) followed by the reduction of cerium in the bulk (high-temperature peak). Therefore, we can assume that low-temperature reduction events are strongly influenced by textural properties such as the specific surface area. Thus, textural properties may explain the presence of the reduction peak at 430 °C only for CP; once this sample has much higher surface area than the sample CC.

The addition of nickel does not interfere in Ce^{4+} reduction process. However, a new main peak at 330 °C is observed in reduction profiles of NCC and NCP samples. This new event can be assigned to the reduction of Ni^{2+} to metallic nickel. It is worth to note that the shape and intensity of this peak in both samples are very similar, indicating that these characteristics depend only on the impregnation method.

3.4. Catalytic activity tests

The catalytic activity of the nickel-based samples was tested for partial oxidation of methane, after the reduction step. A long-term test was carried out at 800 °C for 10 h to investigate the stability of the catalysts. Fig. 4 depicts the CH_4 conversion profiles obtained as a function of the time on stream. It was found that the conversion levels are increasing about 1% and 2% to the samples NCP and NCC during the first hour, respectively (see in the window on bottom-right). This indicates that the catalysts are being activated during this initial period. Then, the CH_4 conversion slightly decreases reaching 77% and 80% after ten hours on stream, respectively. It seems that NCP reaches stability after four hours on stream, while for NCC this is observed only after seven hours. Nevertheless, the NCC catalyst keeps the conversion levels slightly higher than those found for NCP during the entire evaluation period.

The syngas production from CH_4/O_2 mixtures over nickel-based catalysts is characterized by competition between two methane oxidation reactions, partial and complete (Eqs. (5) and (6), respectively). Indeed, the presence of CO_2 in the gas outlet confirms that the total oxidation of methane takes place. This reaction is also responsible for the water formation, which it was condensed and collected during all time on stream. The samples NCP and NCC produced 5.64 and 4.77 g of water, respectively. The selectivities toward CO and CO_2, as well as the H_2/CO ratio, are given in Fig. 5.

For the sample NCP, the H_2/CO ratio remained closer to the

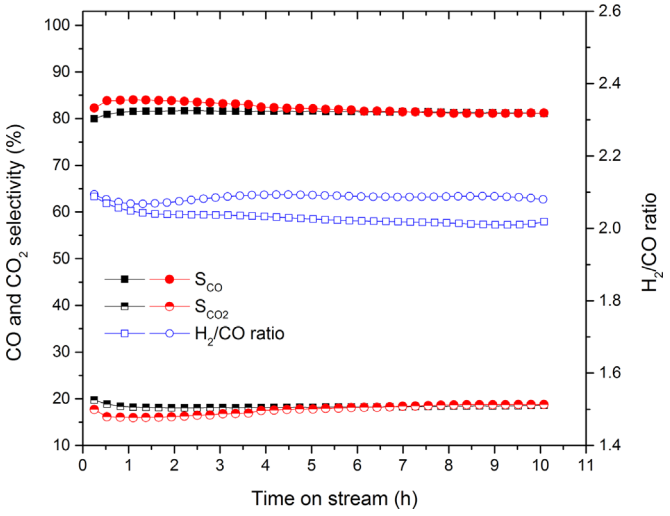

Fig. 5. CO and CO_2 selectivities obtained as a function of the time on stream at 800 °C.

stoichiometric value of 2 compared to what is observed for the sample NCC. It is noted that for the sample NCC the selectivities reached stable values after one hour on stream. On the other hand, the stability of the selectivities observed for the sample NCC was reached only after five hours on stream. After that, both samples come to present identical selectivity values. It seems that, for the sample NCC, during the first five hours on stream, another reaction involving CO, CO_2, H_2 and H_2O takes place, probably the water gas shift (WGS) reaction (Eq. 7). The WGS reaction may explain the lower amount of water collected for the sample NCC as well as the behavior depicted in Fig. 5.

$$CH_4 + ½O_2 \rightarrow 2H_2 + CO \quad (5)$$

$$CH_4 + 2O_2 \rightarrow CO_2 + 2H_2O \quad (6)$$

$$H_2O + CO \rightarrow H_2 + CO_2 \quad (7)$$

Beyond the catalytic reactions mentioned, it is reasonable to admit that other side reactions may take place during syngas production via methane oxidation. These reactions can promote coke formation leading to the catalyst deactivation. However, the catalysts NCC and NCP did not show any significant sign of

deactivation. It is expected that the high oxygen mobility typically shown by Zr-CeO2 compounds improves resistance against coking.

4. Conclusions

In conclusion, we have presented the synthesis of $Ce_{0.75}Zr_{0.25}O_2$ via two different routes: microwave-induced combustion reaction and Pechini. The synthesized samples were impregnated with nickel nitrate and calcined to produce a nanocrystalline composite. XRD results confirmed the crystallization of two cubic phases, NiO, and $Ce_{0.75}Zr_{0.25}O_2$ with fluorite-type structure. Microstructural analysis performed by Rietveld method suggested an isotropic character of the crystallites regardless of the applied synthetic route. The prepared samples exhibit nanocrystalline characteristics, with average crystallite size smaller than 85 nm.

It was noticed that the impregnation process followed by calcination at 900 °C provoked a significant drop in the surface area of the sample prepared by Pechini method from 48 to 18 m^2/g. On the other hand, the sample prepared by self-combustion showed much more stability keeping the same specific surface area of 6 m^2/g. SEM images have revealed that NiO phase is filling the pores of $Ce_{0.75}Zr_{0.25}O_2$ synthesized by self-combustion method and appears on the surface of large agglomerates when prepared by the Pechini method.

Both nickel-based catalysts, NCP and NCC, showed high activity and stability during a long-term test in partial oxidation of methane without any sign of deactivation during the time on stream. Thus, it was found that the main advantages of microwave-induced combustion method compared to Pechine method are its simplicity and low cost, in this case keeping the same catalytic performance.

Acknowledgement

The authors acknowledge the financial support received from funding agency – CAPES (Brazil). We also thank the NEPGN/NUPER/UFRN for the SEM analysis and the Centre for Gas Technology and Renewable Energy (CTGAS-ER) for the catalytic tests.

References

[1] V.D. Sokolovskii, N.J. Coville, A. Parmaliana, I. Eskendirov, M. Makoa, Methane partial oxidation. Challenge and perspective, Catal. Today 42 (1998) 191–195.
[2] N.D. Parkins, C.I. Warburton, J.D. Wilson, Natural gas conversion to liquid fuels and chemicals: where does it stand? Catal. Today 18 (1993) 385–442.
[3] C. Guo, X. Zhang, J. Zhang, Y. Wang, Preparation of La_2NiO_4 catalyst and catalytic performance for partial oxidation of methane, J. Mol. Catal. A: Chem. 269 (2007) 254–259.
[4] H.E. Figen, S.Z. Baykara, Hydrogen production by partial oxidation of methane over Co based, Ni and Ru monolithic catalysts, Int. J. Hydrog. Energy 40 (2015) 7439–7451.
[5] M. Khajenoori, M. Rezaei, B. Nematollahi, Preparation of noble metal nanocatalysts and their applications in catalytic partial oxidation of methane, J. Ind. Eng. Chem. 19 (2013) 981–986.
[6] P.D.F. Vernon, M.L.H. Green, A.K. Cheetham, A.T. Ashcroft, Partial oxidation of methane to synthesis gas, Catal. Lett. 6 (1990) 181–186.
[7] P.D.F. Vernon, M.L.H. Green, A.K. Cheetham, A.T. Ashcroft, Partial oxidation of methane to synthesis gas, and carbon dioxide as an oxidizing agent for methane conversion, Catal. Today 13 (1992) 417–426.
[8] S.C. Tsang, J.B. Claridge, M.L.H. Green, Recent advances in the conversion of methane to synthesis gas, Catal. Today 23 (1995) 3–15.
[9] B.S. Barros, D.M.A. Melo, S. Libs, A. Kiennemann, CO_2 reforming of methane over La_2NiO_4/α-Al_2O_3 prepared by microwave assisted self-combustion method, Appl. Catal. A Gen. 378 (2010) 69–75.
[10] M.R. Cesário, B.S. Barros, C. Courson, D.M.A. Melo, A. Kiennemann, Catalytic performances of Ni–CaO–mayenite in CO_2 sorption enhanced steam methane reforming, Fuel Process. Technol. 131 (2015) 247–253.
[11] Y. Wang, X. Hong, B. Li, W. Wang, D. Wang, Ytria promoted metallic nickel catalysts for the partial oxidation of methane to synthesis gas, J. Nat. Gas Chem. 17 (2008) 344–350.
[12] M. Virginie, M. Araque, A.-C. Roger, J.C. Vargas, A. Kiennemann, Comparative study of H_2 production by ethanol steam reforming on $Ce_2Zr_{1.5}Co_{0.5}O_{8-\delta}$ and $Ce_2Zr_{1.5}Co_{0.47}Rh_{0.07}O_{8-\delta}$: evidence of the Rh role on the deactivation process, Catal. Today 138 (2008) 21–27.
[13] H.S. Hyun-Seog Roh, Ki-Won Potdar, Jae-Woo Jun, Young-Sam Kim, Oh, Carbon dioxide reforming of methane over Ni incorporated into Ce–ZrO_2 catalysts, Appl. Catal. A Gen. 276 (2004) 231–239.
[14] A. Trovarelli, C. Leitenburg, G. Dolcetti, Design bettter cerium-based oxidation catalysts, Chemtech 27 (1997) 32–37.
[15] S. Rossignol, F. Gerard, D. Duprez, Effect of the preparation method on the properties of zirconia–ceria materials, J. Mater. Chem. 9 (1999) 1615–1620.
[16] Y. Song, H. Liu, S. Liu, D. He, Partial oxidation of methane to syngas over Ni/Al_2O_3 catalysts prepared by a modified Sol–Gel method, Energy Fuels 23 (2009) 1925–1930.
[17] J. Chen, Q. Wu, J. Zhang, J. Zhang, Effect of preparation methods on structure and performance of Ni/$Ce_{0.75}Zr_{0.25}O_2$ catalysts for CH_4–CO_2 reforming, Fuel 87 (2008) 2901–2907.
[18] B.S. Barros, R.S. Oliveira, J. Kulesza, V.R.M. Melo, D.M.A. Melo, S. Alves-Jr, Reddish-orange $Ca_{3-x}Al_2O_6$: XEu^{3+} nanophosphors: fast synthesis and photophysical properties, J. Phys. Chem. Solids 78 (2015) 90–94.
[19] M.R. Phadatare, A.B. Salunkhe, V.M. Khot, C.I. Sathish, D.S. Dhawale, S.H. Pawar, Thermodynamic, structural and magnetic studies of $NiFe_2O_4$ nanoparticles prepared by combustion method: Effect of fuel, J. Alloy. Compd. 546 (2013) 315–319.
[20] S. Barison, M. Fabrizio, S. Fasolin, F. Montagner, C. Mortalo, Microwave-assisted sol–gel Pechini method for the synthesis of $BaCe_{0.65}Zr_{0.20}Y_{0.15}O_{3-\delta}$ powders, Mater. Res. Bull. 45 (2010) 1171–1176.
[21] P. Jana, V.A. de la Peña O'Shea, J.M. Coronado, D.P. Serrano, Cobalt based catalysts prepared by Pechini method for CO_2-free hydrogen production by methane decomposition, Int. J. of Hydrogen Energy, vol. 35, 2010, pp. 10285–10294.
[22] A. Chowdhury, S. O'Callaghan, T.A. Skidmore, C. James, S.J. Milne, Nanopowders of $Na_{0.5}K_{0.5}NbO_3$ prepared by the Pechini method, J. Am. Ceram. Soc. 92 (2009) 758–761.
[23] L. Lutterotti, Maud – Materials Analysis Using Diffraction 2.55, 2016, Available from ⟨http://maud.radiographema.eu/⟩. (accessed in 05.06.16).
[24] H. Th, J.L. Keijser, E.J. Langford, A.B.P. Mittemeijer, Vogels, Use of the Voigt function in a single-line method for the analysis of X-ray diffraction line broadening, J. Appl. Cryst. 15 (1982) 308–314.